Chemical Engineering Journal 329 (2017) 220–230

Contents lists available at ScienceDirect

Chemical Engineering Journal

journal homepage: www.elsevier.com/locate/cej

Controlled multiphase oxidations for continuous manufacturing of fine chemicals

Konstantin N. Loponov [a,*], Benjamin J. Deadman [b], Ju Zhu [c], Chris Rielly [a], Richard G. Holdich [a,*], King Kuok (Mimi) Hii [b], Klaus Hellgardt [c]

[a] Department of Chemical Engineering, Loughborough University, Loughborough LE11 3TU, UK
[b] Department of Chemistry, Imperial College London, Exhibition Road, South Kensington, London SW7 2AZ, UK
[c] Department of Chemical Engineering, Imperial College London, Exhibition Road, South Kensington, London SW7 2AZ, UK

HIGHLIGHTS

- Electrochemically generated $S_2O_8^{2-}$ is a viable reagent for biphasic oxidations.
- Reaction times were reduced using membrane emulsification in a dispersion cell.
- Membrane emulsification was successfully integrated with OFR for the first time.
- Continuous extraction in OFR allowed 94% removal of the product in a single pass.

GRAPHICAL ABSTRACT

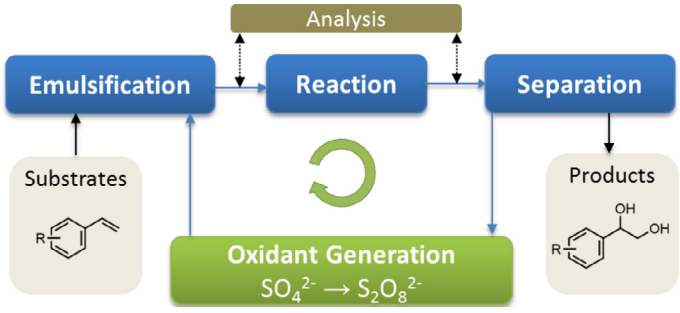

ARTICLE INFO

Article history:
Available online 5 May 2017

Keywords:
Biphasic liquid-liquid oxidation
Process intensification
Flow chemistry
Membrane emulsification
Oscillatory Flow Reactor
Electrochemistry

ABSTRACT

The feasibility of an integrated continuous biphasic oxidation process was studied, incorporating (i) electrochemical generation of an oxidant, (ii) membrane emulsification and an Oscillatory Flow Reactor (OFR) to facilitate mass-transfer in a biphasic reaction system and (iii) product extraction to enable regeneration of the oxidant. The biphasic, organic solvent-free dihydroxylation of styrene by ammonium peroxodisulfate solutions (including electrochemically generated peroxodisulfate) was investigated as a model reaction, both in batch and in an OFR. Heating of peroxodisulfate in a strongly acidic solution was demonstrated to be essential to generate the active oxidant (Caro's acid). Membrane emulsification allowed mass-transfer limitations to be overcome, reducing the time scale of styrene oxidation from several hours in a conventional stirred tank reactor to less than 50 min in a dispersion cell. The influence of droplet size on overall reaction rate in emulsions was studied in detail using fast image capturing technology. Generation of unstable emulsions was also demonstrated during the oxidation in OFR and product yields >70% were obtained. However, the high-frequency/high-displacement oscillations necessary for generation of fine droplets violated the plug flow regime. Membrane emulsification was successfully integrated with the OFR to perform biphasic oxidations. It was possible to operate the OFR/cross-flow membrane assembly in plug flow regime at some oscillatory conditions with comparable overall oxidation rates. No mass-transfer limitations were observed for droplets <60 μm. Finally, the continuous post-reaction separation was demonstrated in a single OFR extraction unit to enable continuous regeneration of the oxidant.

* Corresponding authors.
E-mail addresses: k.loponov@lboro.ac.uk (K.N. Loponov), r.g.holdich@lboro.ac.uk (R.G. Holdich).

http://dx.doi.org/10.1016/j.cej.2017.05.017
1385-8947/

1. Introduction

In recent years, greater awareness of environmental and safety issues has led to increasingly stringent regulatory controls on manufacturing processes, fuelling demand for 'green' chemical technologies that can deliver greater atom, process, and economic efficiency [1]. Currently, chemical technologies adopted in pharmaceutical industries are largely based on multi-purpose batch/semi-batch reactors used in the sequential multi-step synthesis, with each step requiring a further unit of operation for product separation. As a result, the production of fine chemicals and pharmaceuticals suffers from very poor E-factors (mass of waste per mass of product [2], typically 25→100) and high costs. Low space-time yields, insufficient temperature control leading to poor selectivity and difficulties in process control (scale-up in particular) are amongst other disadvantages of batch manufacturing processes. A particular challenge for the pharmaceutical industry is the development of environmentally benign oxidation methods. Oxidation chemistry is currently under-utilised in the pharma manufacturing industry (3.9% of reactions cf. 14% for reductions) due to the difficulties of process implementation at scale, and therefore manufacturing routes avoid oxidation if possible [3]. Nevertheless, benign oxidation methods are listed in the top ten of the most important research areas by the ACS Green Chemistry Institute's Pharma Round Table [1,3].

In order to address these issues, there is growing interest in the development of fully integrated continuous processes for scalable and efficient multi-phase chemical synthesis [4]. Manufacturing in flow reactors confers multiple benefits of process intensification, scalability and novel opportunities in process design and control [4–11]. Moreover, in a recent survey of key green engineering research areas, 'continuous processing' was identified as the top priority for delivering improved cost-effectiveness, quality, safety and environmental standards to the pharmaceutical industry [12]. This research aims to develop an integrated scalable continuous process that can offer an elegant, safe, atom- and energy-efficient solution to biphasic liquid-liquid oxidation reactions. The modular process includes (i) continuous electrochemical generation of synthetically useful concentrations of oxidant; (ii) an advanced flow chemistry system based on process intensification technology capable of resolving mass-transfer limitations in biphasic oxidations; and (iii) facile post-reaction separation to enable recycling of the oxidant.

Peroxodisulfates ($S_2O_8^{2-}$) are among the strongest and environmentally safe oxidants (E = 2.01 V vs. SHE). Compared to unstable peroxides and peracid reagents that are generally employed as diluted solutions, it is safe to handle peroxodisulfate both as a solid and as an aqueous solution under ambient conditions. Recently, it was demonstrated, using a commercial electrolytic flow cell with a boron-doped diamond anode, that it is possible to continuously generate solutions of ammonium peroxodisulfate on-site and on-demand [13]. This work focuses on the development of process intensification technology for efficient biphasic oxidations using peroxodisulfates, including continuous product separation.

In order to deliver adequate reaction rates in a flow reactor, it is necessary to overcome mass transport limitations of immiscible liquids in a biphasic liquid-liquid system. This can be achieved by the formation of thermodynamically unstable fine emulsions with sufficient interfacial area. For this purpose, the synergy was utilised between continuous pulse-flow membrane for generation of emulsions with an oxidant in the aqueous phase and a reactant in the organic phase and mesoscale Oscillatory Flow Reactor (OFR) with smooth periodic constrictions for multiphase reactions.

Membrane emulsification is one of the most efficient methods for generation of emulsions with low energy requirements which allows the production of controllable, narrowly distributed micro-droplets [14,15]. Recently, it has been demonstrated that a continuous cross-flow system operated under pulsed flow conditions can provide up to 45% v/v dispersed phase content in a single overall pass [16]. Moreover, this system can be coupled with an OFR to provide sufficient interfacial area and residence time for performing biphasic reactions. To the best of our knowledge, this is the first time an OFR has been integrated with a cross-flow membrane emulsification.

The OFR is a tubular reactor with periodically spaced compartments separated by inner structures, such as baffles or smooth periodic constrictions [17–20], to provide mixing via the generation and extinction of eddies created by the interaction of flow oscillations with the constrictions [17–19]. Thus, each compartment of an OFR acts as a Continuous Stirred Tank Reactor (CSTR) and a small steady flow component allows a required residence time to be obtained [20–22]. Owing to excellent axial and radial mixing in each compartment, these reactors provide a better alternative reactor for a wide range of processes such as continuous crystallisation, biphasic production of biodiesel and suspension polymerisation [20,21,23].

Post-reaction separation can be achieved via coalescence of the unstable emulsion into two phases or extraction in the case of water-soluble products. Potentially, the poor atom efficiency of peroxodisulfate solutions can be mitigated by electrochemical regeneration of the sulfate byproduct back to peroxodisulfate after product separation. Thus, the proposed methodology can provide a greener and more efficient route to the multiphase oxidations of alcohols and alkenes (including epoxidations) which is demonstrated using oxidation of styrene as a case study reaction.

2. Methods

2.1. Chemicals

All reagents were used as received without further purification: deionised water (18 MΩ cm), $(NH_4)_2S_2O_8$ (98%, Sigma-Aldrich and Acros), H_2SO_4 (96%, Fisher Scientific and VWR), H_2O_2 (30% w/w in H_2O, VWR), $KHSO_5{\cdot}0.5KHSO_4{\cdot}0.5K_2SO_4$ (Merck), sodium dodecyl sulfate (≥99%, Sigma-Aldrich), IGEPAL® CA-720 (Sigma-Aldrich), styrene (≥99%, Sigma-Aldrich and Acros), 1-Phenyl-1,2-ethanediol (97%, Sigma-Aldrich and Merck), $(NH_4)_2SO_4$ (≥99%, Sigma-Aldrich), ethyl acetate (99% Acros Organics), *meso*-tetraphenyl porphyrin (≥99%, Sigma-Aldrich), isopropanol (≥99.7%, Sigma-Aldrich).

2.2. Batch oxidations of styrene

A solution of 1 M or 0.4 M $(NH_4)_2S_2O_8$ (50 mmol) in 2 M H_2SO_4 (50 mL) was pre-heated at 50 °C for 16 h in a 250 mL 3-neck round-bottomed flask (80 mm diameter). Potassium peroxomonosulfate triple salt (a stabilised salt form of Caro's acid, $KHSO_5{\cdot}0.5KHSO_4{\cdot}0.5K_2SO_4$) and H_2O_2 were used directly without thermal pre-treatment. After the pre-treatment, the oxidant solution was allowed to cool until the aluminium heating mantle stabilised at 50 °C, before styrene (20 mmol) was added and the vessel stirred at 600 rpm by a PTFE half-moon stirrer blade (52 mm diameter, impeller Re = 27,040). The mantle temperature was maintained at 50 °C for up to 6 h during which time the reaction progress was measured by HPLC analysis of samples taken periodically.

2.3. Oxidation of styrene in dispersion cell reactor

Oxidation of styrene was carried out in a dispersion cell (Micropore Ltd) designed for low energy controllable generation

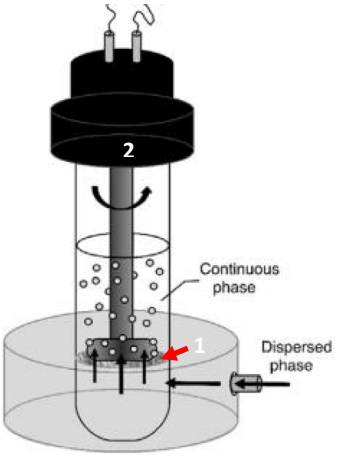

Fig. 1. Diagram of the dispersion cell (Micropore). For more details see Section 2.3.

of emulsions (see Fig. 1) [15,24]. The dispersion cell consists of two cylindrical compartments, a small 4 mL compartment at the bottom of the cell for the dispersed phase and a large glass compartment of 3.8 cm internal diameter (150 mL) at the top for the continuous phase. The two compartments are separated by a flat micro-sieve stainless steel membrane (1) with a circular area of 5 μm pores (total area of the porous ring is 1.85 cm^2 and surface porosity is 0.19%). The compartment at the bottom of the cell is equipped with the inlet port for injection of the dispersed phase into a continuous phase through the membrane. Above the membrane, there is a double-bladed paddle stirrer (blade diameter is 3 cm) equipped with 24 V DC motor (2) which produces shear stress at the surface of the membrane for droplet detachment during rotation. Thus, droplet size for a particular system can be controlled by the injection rate of the dispersed phase, rotation speed and pore diameter of the membrane.

An aqueous solution of 1 M $(NH_4)_2S_2O_8$ in 2 M H_2SO_4 (100 mL) was pre-heated for 18 h at 50 °C before it was used as the continuous phase in the reaction. Pure styrene was injected through the membrane at a flow rate of 0.25 mL min^{-1} for 18.3 min using a syringe pump (The New Era). The total volume of the injected styrene was 4.575 mL. The corresponding ratio of $S_2O_8^{2-}$ to styrene in the dispersion cell was 2.5:1 after the injection. Three different rotation speeds were used for the generation of emulsions (218, 555 and 1246 rpm, corresponding Re numbers are 1635, 4163 and 9345) and the dispersion cell was thermostated at 50 °C during all the experiments. In some experiments, sodium dodecyl sulfate, SDS (2 mg mL^{-1}) or Igepal 720, IGP (0.1 mg mL^{-1}) were added to the continuous phase prior to the reaction in order to stabilise the droplets. Images of the emulsions and droplet size distributions were measured by a Visual Process Analyser, ViPA (Jorin). Samples (1 mL) were taken at regular intervals during the oxidation and injected into 50 mL of 0.2% wt. IGP dissolved in styrene-saturated water and recirculated through ViPA flow cell. In parallel, 0.3 mL samples were diluted twice with isopropanol and conversions were measured using HPLC.

2.4. Oxidations of styrene in OFR

Continuous oxidation of styrene was carried out in the OFR Rig (Fig. 2) consisting of a flow oscillator (1) (custom-built bellows pump with the flow oscillations range of 1–10 Hz and displacement of 0–3 mL, Williamson Manufacturing Company) and a set of 5 consecutively connected jacketed tubular glass flow reactors (4). Each tube has a volume of 27 mL and contains 16 periodically spaced bubble-shaped compartments with smooth periodic constrictions (bubble length is 14 mm, the maximum bubble diameter is 15 mm, constriction between bubbles diameter is 5 mm, and the volume is 1.5 mL, see the inset in Fig. 2). The total length and volume of the reactor rig are 152 cm and 135 mL correspondingly. The reactor is equipped with sample ports (P0-P4) situated along the reactor between the tubular sections. Dispersed and continuous phases (styrene and oxidant) were supplied to the reactor by a VICI pump (**2**). Styrene was continuously pumped into the reactor via a PTFE capillary (1 mm ID) inserted into the first bubble-shaped segment of the OFR via a custom made T-connection attached to the inlet of the reactor (**5**) and product was collected from the outlet (**6**). The rig was thermostated at 50 °C during all the oxidation tests using a recirculating heating bath (**3**).

Aqueous solutions of 1 M $(NH_4)_2S_2O_8$ in 2 M H_2SO_4 (1 L) were pre-heated for 18, 24 or 30 h at 50 °C before they were used as the continuous phase in the reaction. Flow rates, space residence times, molar ratios of peroxodisulfate to styrene, corresponding frequencies of oscillations and displacements and corresponding net flow and oscillatory Reynolds numbers as well as Strouhal numbers ($Re_n = vD\rho/\mu$, $Re_0 = 2\pi x_0 fD\rho/\mu$, and $St = D/4\pi x_0$, where v is superficial velocity, f is the frequency of oscillations, x_0 is the centre-to-peak amplitude of the displacement, D is an effective diameter, ρ is the density of the liquid, and μ is kinematic viscosity [20,25]) are summarised in Table 1, entries 1–3. Slow flow rate experiments were performed with total flow rates of 1.127 mL min^{-1} or 1.295 mL min^{-1} (entries 1 and 2) while fast flow rate experiments were performed with at total flow rate of 6.495 mL min^{-1} (entry 3). Samples (1 mL for HPLC analysis and 3 mL for ViPA analysis of droplet size distributions) were taken from ports P0-P4 and analysed following the method described in Section 2.3.

Residence time distributions (RTDs) were measured in a water-styrene system with 37.5 mg L^{-1} IGP surfactant added to the aqueous phase for stabilisation of the microdroplets. This amount of surfactant provides an interfacial tension of about 14.2 mN m^{-1} in the biphasic system which is similar to that in the reaction mixture after the conversion of half of the styrene into the product diol. Standard tracer experiments [26] were performed using short pulse injections (<1 s) of 0.3 mL water-styrene emulsions, containing tetraphenyl porphyrin dye, into sample ports P0-P4. A short time of injection ($\Delta t_{inj} \ll t = V_R/u_\Sigma$) and low injection volume ($\Delta V_{inj} \ll V_R$) provide a good approximation to Dirac impulse injection, δ(t) and therefore this method provides the internal RTD function via direct measurement of tracer concentration at the outlet of the OFR. A custom-made fluorescence cell, connected by an optical fibre to a USB2000 + XR1-ES UV–VIS spectrometer (Ocean Optics), was used for this purpose and the concentration of the tracer was followed by dye fluorescence at 650 nm. Residence times were calculated from the RTDs as first moments, $\tau = \int t \cdot f(t)dt$. Quantitative analysis of oxidising species (Caro's acid) in the preheated oxidant was performed using recently developed redox colorimetry assays (unpublished results).

2.5. Cross-flow membrane emulsification module

A cross-flow membrane emulsification module was provided by Micropore (see Fig. 3). The module consists of a stainless steel tubular case (**1**) with the inlet for the dispersed phase (styrene) (**2**), two compression fittings with ferrules and nuts (**3**) and two stainless steel tubular segments (**4**) with grooves and O-rings (**5**) for holding a Shirasu Porous Glass (SPG) tubular membrane (**6**) (L = 10 cm, ID = 8 mm, wall thickness of 1 mm, average pore size of 10 μm, SPG Technology). The membrane assembly was situated vertically, with an inlet for the continuous phase (**7**) connected to the outlet tube of the bellows flow oscillator and the outlet of the

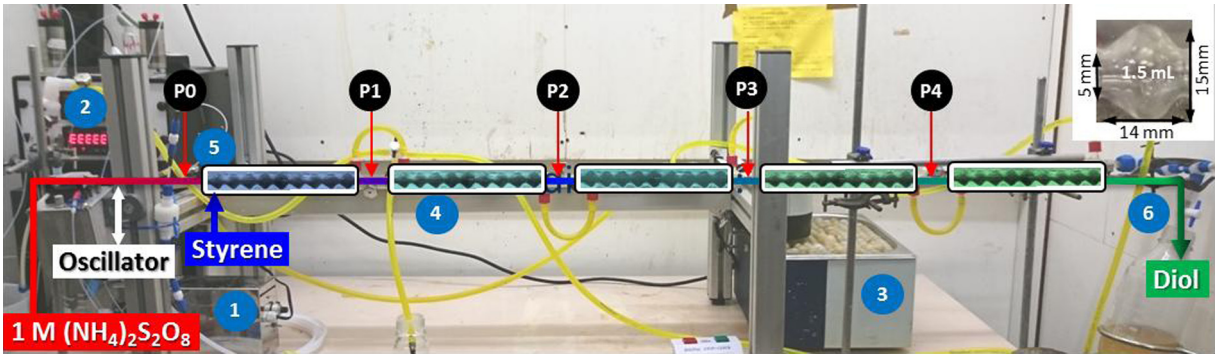

Fig. 2. Photo of the OFR rig with component scheme overlay.

Table 1
Flow rates of the dispersed and continuous phases, corresponding space residence times in the OFR, frequencies of flow oscillations and displacements.

N	n_{PS}:n_{ST}	u_{org}, mL min^{-1}	u_{aq}, mL min^{-1}	u_{Σ}, mL min^{-1}	$t = V_R/u_{\Sigma}$, min	f, Hz	ΔV, mL	x_0, m	Re_n	Re_0	St
1	2.4:1	0.051	1.076	1.127	119.8	8	1.4	0.008	2.3	5231	0.12
2	2.8:1	0.051	1.244	1.295	104.2	8	1.4	0.008	2.6	5231	0.12
						8	0.8	0.004		2615	0.23
3	2.8:1	0.255	6.220	6.495	20.8	8	1.4	0.008	13.3	5231	0.12
						8	0.8	0.004		2615	0.23
						5	1.0	0.005		1923	0.20
						5*	0.4*	0.002		865	0.44
						8*	0.4*	0.002		1385	0.44
						10*	0.3*	0.001		1038	0.74

* OFR integrated with cross-flow membrane emulsification module; n_{PS}:n_{ST} is a molar ratio of peroxodisulfate to styrene, V_R is reactor volume, ΔV is displacement volume, u_{org} and u_{aq} are flow rates of organic and aqueous phases, u_{Σ} is total flow rate, f is the frequency of flow oscillations, x_0 is maximum liquid displacement during the oscillation, Re_n and Re_0 are net flow and oscillatory Reynolds numbers, St is Strouhal number.

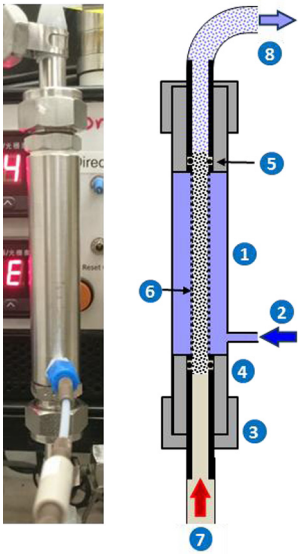

Fig. 3. Photo and scheme showing the cross-flow membrane emulsification module.

membrane emulsification module (**8**) connected to the OFR by a PTFE elbow tubular connection.

An aqueous solution of 1 M $(NH_4)_2S_2O_8$ in 2 M H_2SO_4 (1 L) was first heated for 18 h at 50 °C before IGP was added to make a 150 mg L^{-1} surfactant solution for stabilisation of the droplets. The solution was then pumped using a VICI pump with the superimposed oscillations of flow through the inner space of the SPG membrane emulsification module. Pure styrene was pumped through the membrane by the VICI pump. The emulsion was generated at room temperature and the oxidation of styrene was carried out at 50 °C in the OFR. Corresponding flow rates of continuous and dispersed phases, space residence time, the molar ratio of persulfate to styrene, frequencies of flow oscillations and displacements are shown in Table 1, entry 3. Droplet size analysis and RTDs were measured in a similar manner to that described in Section 2.5.

2.6. Continuous extraction of the diol

Continuous extraction of the diol product was carried out in a smaller volume OFR at 20 °C (V_R = 12 mL). A solution mimicking the composition of the reaction mixture after the completion of the oxidation (0.3 M of 1-phenyl-1,2-ethanediol, 2 M H_2SO_4 and 2 M $(NH_4)_2SO_4$) was pumped through the OFR at different flow rates using the VICI pump. At the same time, ethyl acetate was pumped to the inlet of the OFR (see Table 2 and Fig. 4 for more details). The aqueous phase flow was oscillated at a frequency of 5 Hz with 1.2 mL displacement using a custom-built bellows pump (Williamson Manufacturing Company). The amount of the diol extracted from the aqueous phase was measured by HPLC.

3. Results and discussion

3.1. Oxidation of styrene in a stirred tank batch reactor

The dihydroxylation of styrene by ammonium peroxodisulfate was chosen as a model biphasic oxidation process in this study (Fig. 5).

During the early development of this reaction in a stirred tank reactor, an induction period was observed in the conversion of styrene to its diol (Fig. 6). The reaction of styrene with freshly prepared 1 M solutions of ammonium peroxodisulfate proceeded

Table 2
Flow rates of the aqueous phase and ethyl acetate (EA), corresponding volume ratios and space residence times in the OFR reactor tested in the extraction of the diol product.

V_{EA}:V_{aq}	U_{aq}, mL min^{-1}	u_{EA}, mL min^{-1}	u_{Σ}, mL min^{-1}	$t = V_R/u_{\Sigma}$, min
1:1	0.648	0.648	1.296	9.3
1:1	1.295	1.295	2.590	4.6
1:1	2.590	2.590	5.180	2.3
1:1	3.885	3.885	7.770	1.5
1:2	0.648	1.295	1.943	6.2
2:1	2.590	1.295	3.885	3.1
3:1	3.885	1.295	5.180	2.3
2:1	3.453	1.727	5.180	2.3
1:2	1.727	3.453	5.180	2.3
1:2	0.863	1.727	2.590	4.6
2:1	1.727	0.863	2.590	4.6

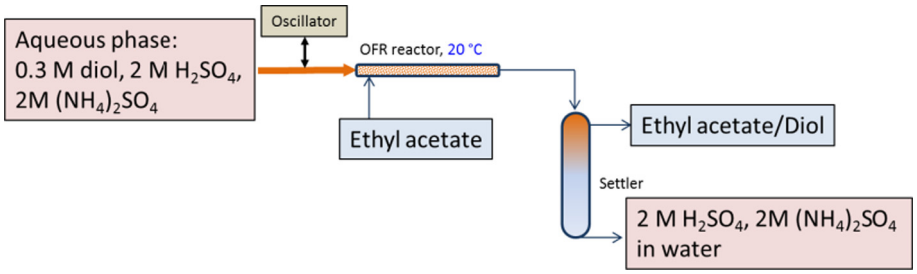

Fig. 4. Scheme describing the continuous extraction of the diol by ethyl acetate using an OFR.

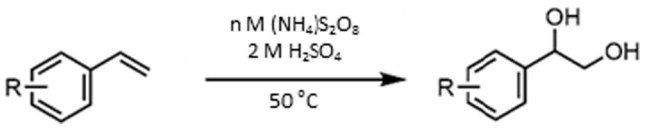

Fig. 5. The dihydroxylation of styrene by ammonium peroxodisulfate.

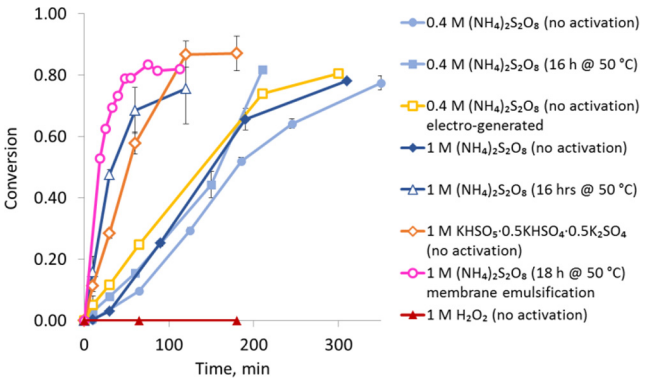

Fig. 6. Effect of oxidant type, its concentration and pre-treatment methods (shown in brackets) on the rate of styrene oxidation carried out in a stirred tank reactor at 50 °C. Oxidation in the dispersion cell reactor using membrane emulsification is shown for comparison.

slowly over the first 30 min before the rate of diol formation increased and a maximum conversion (ca. 80%) was achieved after 6 h. Strongly acidic conditions were found to be necessary for the effective oxidation of styrene by peroxodisulfate. Under pH neutral conditions the oxidation was extremely slow and produced multiple by-products. It was also found that higher reaction temperatures (70–90 °C) accelerated the oxidation of styrene by acidic solutions of peroxodisulfate but at the expense of product yield and purity which were both reduced. In order to inhibit the undesired side reactions, all further oxidations were performed at 50 °C. It was subsequently found that preheating the acidic ammonium peroxodisulfate solution (50 °C for 16 h) accelerated the rate of styrene dihydroxylation, eliminating the induction period and reducing the reaction time to <2 h (Fig. 6). The preheated peroxodisulfate solution oxidised styrene at a similar rate as solutions of the potassium peroxomonosulfate triple salt, a commonly used oxidant in organic synthesis (Fig. 6). It has been reported that acidic solutions of peroxodisulfate undergo thermal decomposition to form peroxomonosulfate [27,28]. The observed induction period when using peroxodisulfate as the oxidant, and the improved reactivity of preheated peroxodisulfate solutions suggested that the dihydroxylation of styrene by peroxodisulfate actually proceeds via the generation of a peroxomonosulfate species as the oxidising agent. For the purposes of this study, a pre-treatment regime of 16 h at 50 °C was used to activate the peroxodisulfate solutions and ensure that the dihydroxylation of styrene was not rate limited by the in situ generation of peroxomonosulfate. A detailed analysis of the underlying reaction processes in the dihydroxylation of styrenes by peroxodisulfate is the subject of ongoing research and will be reported in due course.

For comparison, the oxidation was also performed using a solution of peroxodisulfate (0.4 M) generated by an electrochemical cell [13] (Fig. 6). In this case, the electrochemically generated peroxodisulfate (non-activated) appeared to be as reactive as the commercially procured peroxodisulfate of the same concentration (after it was activated at 50 °C for 16 h). It has previously been reported that electrochemically generated peroxodisulfate solutions were effective oxidants in organic transformations [29].

Assuming the reaction occurs at the interface, it was postulated that it should be possible to accelerate the reaction by performing the oxidation in micron-size emulsions, capitalising on their large interfacial area. For example, in the case of biphasic catalytic epoxidation of sunflower seed oil by hydrogen peroxide, no significant mass-transfer limitations were observed for average droplet sizes less than 15 μm [30,31]. To test this approach, the oxidation of styrene was carried out using energy efficient membrane emulsification in a dispersion cell (Fig. 1) and the result can be seen in Fig. 6. As expected, the efficient dispersion of styrene led to a nearly twofold increase in the initial oxidation rates (from

8×10^{-5} M s^{-1} in stirred tank to 1.4×10^{-4} M s^{-1} in the dispersion cell).

3.2. Oxidation of styrene in dispersion cell

Following the promising results of the application of membrane emulsification to biphasic oxidations, a more detailed study of styrene oxidation was performed in a dispersion cell and the results can be seen in Fig. 7. At a rotation speed of 555 rpm, 7 μm droplets of styrene were generated (images of droplet size distributions measured by ViPA are shown in Fig. 7a). This average droplet size is considerably smaller than the 49 μm droplets predicted for this rotation speed and pore diameter by force balance model developed for emulsification in a dispersion cell [15,24]. The discrepancy could be due to the effect of multiple dripping from a single pore leading to the formation of much smaller droplets. Fast oxidation during the injection time (18.3 min) can also lead to the decreased droplet sizes as the first samples were taken for the analysis after styrene injection had completed, when nearly 20% of it had already been oxidised to the diol and dissolved in the aqueous phase. Additionally, rapid coalescence of the unstable emulsion into two phases was observed after the injection, which could lead to the statistics missing large droplets. The addition of a small amount of sodium dodecyl sulfate (below critical micelle concentration) stabilised the droplets leading to a faster overall reaction rate during styrene injection as can be seen in the case of 555 rpm (Fig. 7c). It should be noted here that the diol itself also has surfactant properties. According to our measurements, if half of the styrene is oxidised, the interfacial tension in styrene-peroxodi sulfate/sulfuric acid system decreases from 27.7 to 14.2 mN m^{-1} at 50 °C due to the formation of the diol. Still, rapid coalescence at this rotation speed led to the formation of a separate layer of the organic phase after the injection of styrene. The corresponding decrease of the interfacial area resulted in a significant reduction of the overall reaction rate and maximum conversion of styrene to the diol did not exceed 60% after two hours of oxidation as can be seen in Fig. 7c. It is worth mentioning that it was not possible to measure the droplet size distributions at 218 rpm due to the fast coalescence of the droplets during styrene injection, and the dramatically decreased interfacial area resulted in a very low reaction conversion.

At rotation speeds larger than 1200 rpm, smaller droplets of about 5 μm were detected after the injection of styrene (see Fig. 7b) while the membrane emulsification model predicts average droplet sizes of about 26 μm [15,24]. Again, multiple dripping from a single pore and oxidation of styrene during the injection stage can be the reasons for the discrepancy between the expected and the observed droplet sizes. At these rotation speeds, up to 50% of styrene was converted to the diol during the injection step (see Fig. 7c) and a coalesced bulk phase of styrene was not formed after the injection indicating that the reduction of droplets size due to the oxidation of styrene is faster compared to their coalescence. Complete oxidation of styrene to the diol observed in the next 30 min with a selectivity >80% leads to a complex system where the diol is partly dissolved in the aqueous phase and partly remains as fine and stable dispersion including other less soluble by-products such as 1-phenyl ethanol. At the same time, the addition of surfactants had some hindering effect on the initial overall oxidation rate but did not significantly influence the maximum yield of the diol.

3.3. Oxidation of styrene in OFR

3.3.1. Oxidation at slow flow rates

The model biphasic reaction, developed in the dispersion cell reactor with membrane emulsification, was then transferred into a continuous OFR (Fig. 2). In order to generate unstable emulsions in this assembly, it was necessary to determine the optimal operational regimes for the reactor, which can provide enough energy for the efficient breakage of the organic phase to produce an unstable fine emulsion and to prevent its coalescence until the completion of the reaction. Following the results obtained in batch and dispersion cell tests, a timescale of two hours was initially selected for the reaction (t_Σ = 119.8 min, see Table 1, entry 1). After preliminary tests of different oscillatory conditions, a frequency of 8 Hz and displacements of 1.7 or 0.8 mL were selected to generate adequate flow oscillations for the effective breakage of the droplets inside the OFR; displacements <0.8 mL at this frequency were not enough for the efficient breakage of bulk styrene phase into small droplets, and segregation of two phases was observed. Also, oscillatory frequencies <5 Hz were insufficient to maintain fine emulsions inside the OFR.

OFRs are fully characterised by net flow and oscillatory Reynolds numbers, Re_n and Re_0, describing the intensity of mixing applied to the reactor, and Strouhal number measuring the effective eddy propagation inside the compartments [20,25]. According to the literature, two different regimes of operation exist for baffled reactors. In the region of "soft" mixing, where $50 < Re_0 < 500$ (upper boundary depends on dimensions of reactor and type of baffles) a reasonably good approximation to the plug flow regime is normally observed [20,25,32]. The ratios $\psi = Re_n/Re_0$ are in the range between $2 < \psi < 12$ for this regime [20]. In the case of Re_0 >5000, a fully turbulent regime exists, corresponding to the mixed flow and the reactor is approximated by a single CSTR [25,32]. In

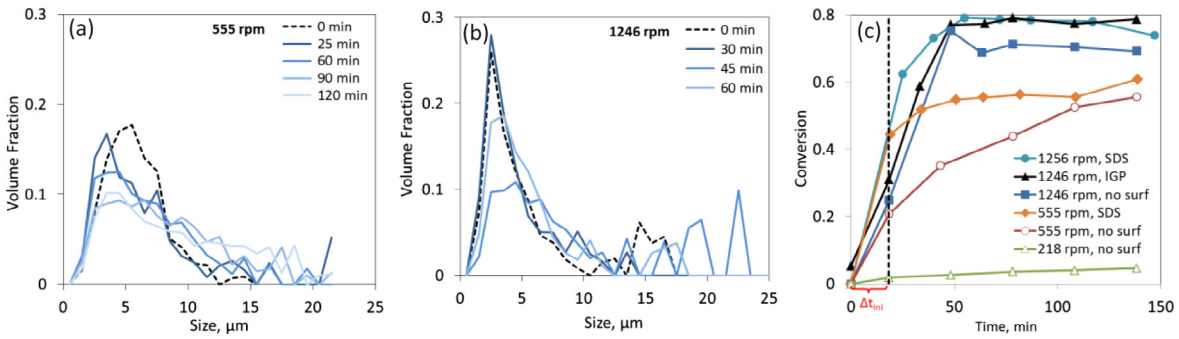

Fig. 7. Droplet size distributions measured by ViPA at different reaction times during the oxidation of styrene in the dispersion cell at 50 °C and rotation speeds of 555 (a) or 1246 rpm (b) without surfactant and conversions at different RPMs (c). The pore size of the stainless steel flat disc membrane was 5 μm. The continuous phase is 1 M $(NH_4)_2S_2O_8$ in 2 M H_2SO_4, 100 mL (pre-heated for 18 h at 50 °C prior to reaction with styrene). Dispersed phase was styrene, injection rate was 0.25 mL min^{-1}; total injected volume was 4.575 mL, $S_2O_8^{2-}$: styrene = 2.5:1. Times in (a) and (b) count after styrene injection ended, vertical dash line in (c) represents the completion of styrene injection (Δt_{inj} = 18.3 min). SDS is sodium dodecyl sulfate (2 mg mL^{-1}), IGP is Igepal 720 (0.1 mg mL^{-1}).

the intermediate region, the flow is not fully mixed, representing a transition between plug flow and CSTR regimes. High St numbers (St >0.2) indicate insufficient eddy generation to effectively mix the compartment, whilst St <0.13 indicate intense eddy formation and propagation into the neighbouring compartments [20]. It is worth mentioning that these ranges were only confirmed for monophasic flows and optimal oscillatory conditions will depend not only on the internal geometry of the reactor but also on the physico-chemical properties of the liquid-liquid dispersion. In our case, Re_0 of 5231 and 2615 were calculated for 1.7 or 0.8 mL displacements at 8 Hz and Reynolds numbers ratios, ψ were found to be about 1979 and 989. These numbers indicate that there is a high degree of back-mixing in the OFR and that the operating regime is far from the acceptable approximation to plug flow [25,32]. The non-plug flow operating regime was further confirmed by RTD analysis (see Fig. 8a, b). St numbers of 0.12 and 0.23 evidence that there are efficient eddy generation and propagation into the adjacent cavities [20].

However, maintaining a large interfacial area in the OFR with biphasic systems is a very challenging task when the reactor operates in a "soft" plug flow regime. The energy of the oscillations is often not enough for the efficient breakage of bulk organic phase to micro-droplets and coalescence dominates in the system. In this case, a special design of OFR (baffles, in particular) may be required in order to fulfil both conditions. For example, biodiesel production is a biphasic process and Re_0 of typically 700 ($\psi \approx 18$) were necessary for good mixing in a standard baffle reactor [33]. The operational regime was further improved using axially oriented sharp-edged helical baffles which allowed efficient mixing at lower Re_0 and operation in plug flow regime [34,35]. Longer reactors and faster flow rates can also improve the performance of the system. Faster flow rates lead to an increase of Re_n and therefore to lower ψ, providing better operation regime of the OFR (closer to plug flow), while a longer reactor will allow sufficient residence time, enough for the complete transformation of styrene to its diol when using the faster flowrate. However, the system studied was limited in terms of operating ranges that can be delivered by the available length and internal geometry of the OFR and those parameters were fixed in this work.

Droplet size distributions of reaction mixture emulsions recorded at steady state, at ports P1-P4 using ViPA, are shown in Fig. 9a and b. It is apparent that for both the displacements studied, the droplet size distributions are virtually unchanged along the reactor. In the case of 0.8 mL displacements, there is a fraction of larger droplets in the droplet size distributions, starting from about 25 μm, indicating that less power is introduced into the reactor during the operation. Average droplet sizes along the reactor were found to be about 12 ± 1 and 17 ± 2 μm for 1.7 and 0.8 mL displacements respectively.

HPLC analysis of the samples taken from the P1 sample port (t_1 = 20.8 min) revealed that up to 95% styrene had already been oxidised to the diol in the first segment of the reactor rig (see Fig. 10a). Complete disappearance of styrene was observed at the P3 sample port. A decreasing amount of styrene and the nearly constant amount of the diol in the reactor, measured at ports P1 and P2, could be due to the partial accumulation of styrene in the first compartments of the reactor rig before it breaks efficiently into smaller droplets. The corresponding conversions of styrene to the diol are nearly constant along the reactor and a conversion level of styrene to the diol of 59 ± 1% was achieved in the case of SO_5^{2-}: styrene molar ratio of 1.7:1 and a space residence time of 2 h (see Table 1, entry 1). Average values of 71 ± 1% and 66 ± 3% for 1.7 and 0.8 mL displacements were obtained at slightly higher SO_5^{2-}: styrene molar ratio (2:1) and shorter space residence time of 1.7 h (see Table 1, entry 2). A lower SO_5^{2-}: styrene ratio of 1.5:1 led to a higher level of unconverted styrene in the sample

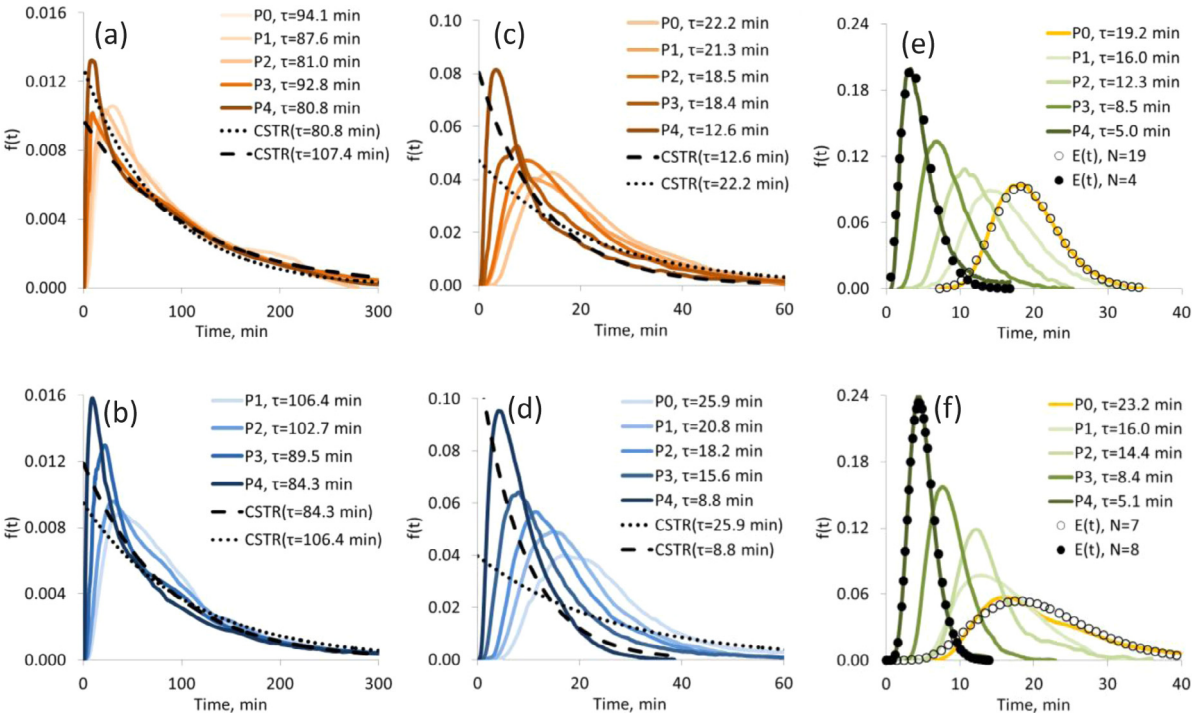

Fig. 8. Residence time distributions in OFR (a–e) and in OFR integrated with the cross-flow membrane module (e, f) for a water-styrene system with Igepal 720 surfactant (37.5 mg L^{-1}) measured at 50 °C by monitoring the response at the outlet of the OFR from the fluorescent tracer injected into P0–P4 ports. Oscillation frequencies are 8 Hz (a–d), 5 Hz (e), 10 Hz (f) and displacements are 1.4 mL (a, c), 0.8 mL (b, d), 0.4 mL (e) and 0.3 mL (f). Flow rates of water are 1.244 mL min^{-1} (a, b) and 6.220 mL min^{-1} (c–f); flowrates of styrene are 0.051 mL min^{-1} (a, b) and 0.255 mL min^{-1} (c–f). Residence times were calculated as first central moments, $\tau = \int t \cdot f(t) dt$, dotted and dashed lines denote RTD in CSTR for the residence times corresponding to P0 and P4.

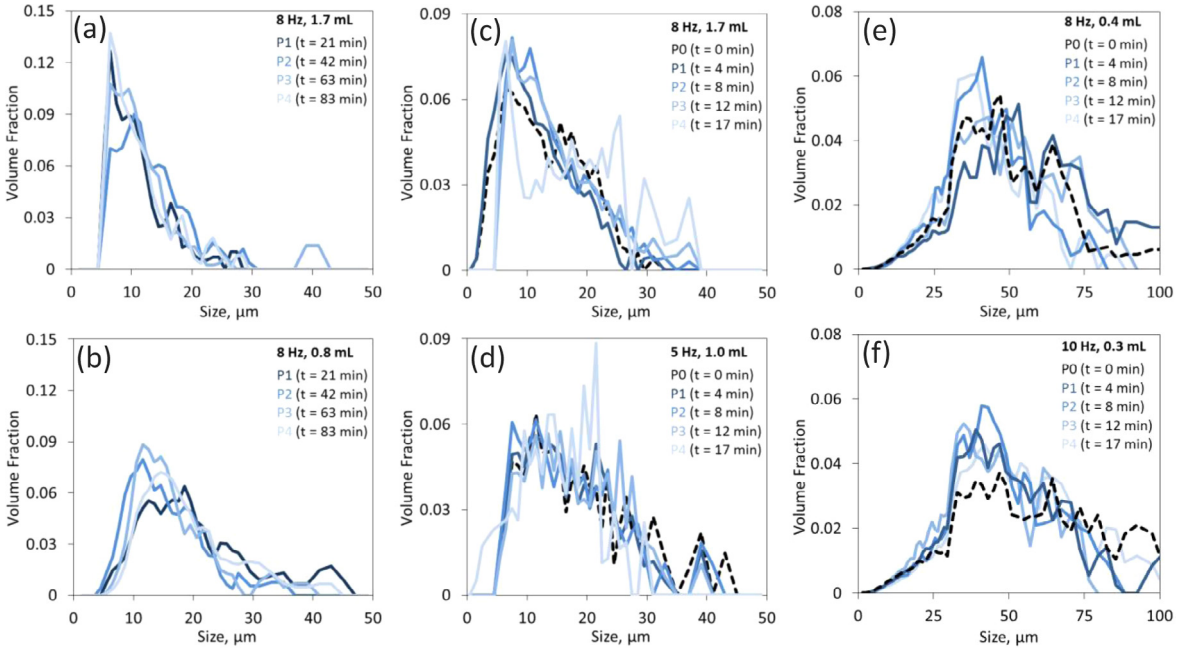

Fig. 9. Droplet size distributions of styrene emulsions measured by ViPA during the oxidation in OFR (a–d) and in OFR integrated with the cross-flow membrane module (e, f). Frequencies: 8 Hz (a–c, e) 5 Hz (d) and 10 Hz (f); displacements: 1.4 mL (a, c), 1 mL (d), 0.8 mL (b), 0.4 mL (e) and 0.3 mL (f). Continuous phase is 1 M $(NH_4)_2S_2O_8$ in 2 M H_2SO_4, flow rates are 1.244 mL min^{-1} (a, b) and 6.220 mL min^{-1} (c–f). Dispersed phase is styrene, flow rates are 0.051 mL min^{-1} (a, b) and 0.255 mL min^{-1} (c–f). A 150 mg L^{-1} Igepal 720 was used in membrane emulsification. Samples were taken from P1–P4 sample ports. Molar ratio $S_2O_8^{2-}$: styrene = 2.8: 1, $t = V_R/u_\Sigma$, T = 50 °C in the reactor.

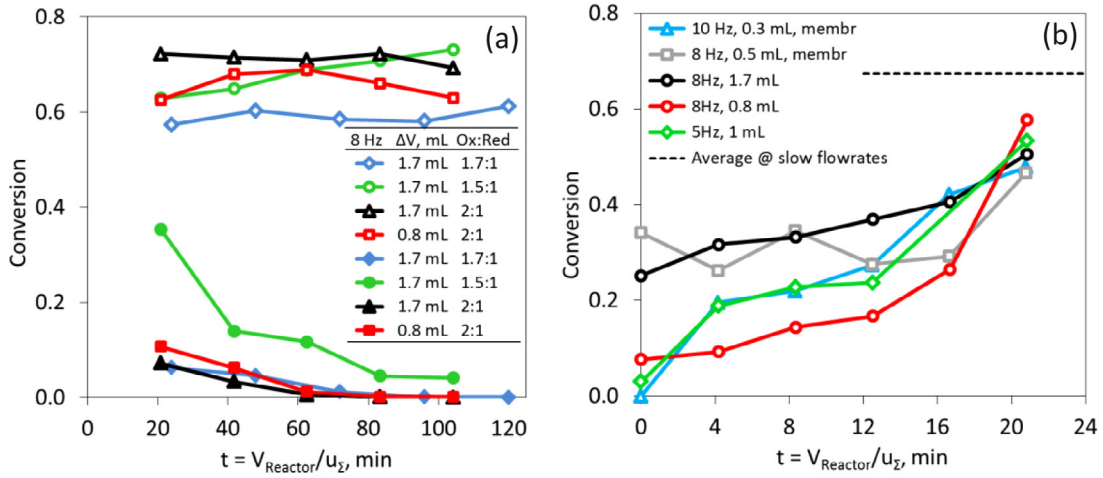

Fig. 10. Biphasic oxidation of styrene (filled markers) to the diol (empty markers) in OFR at 50 °C at different oscillation frequencies and displacements. Samples were taken from P0–P4 sample ports and the outlet of the reactor. Continuous phase is 1 M $(NH_4)_2S_2O_8$ in 2 M H_2SO_4, flow rates are 1.074 mL min^{-1} (diamonds) and 1.244 mL min^{-1} (triangles, squares and circles) (a) and 6.220 mL min^{-1} (b); dispersed phase is styrene, flow rates are 0.051 mL min^{-1} (a) and 0.255 mL min^{-1} (b). Molar ratios SO_5^{2-}:styrene in the reactor are shown as Ox:Red ratios (a). Dash line represents the average level of conversions at slow flow rates, triangles and squares in (b) denote oxidation in OFR with the integrated cross-flow membrane emulsification.

ports and at the outlet of the reactor meaning that there is not enough oxidant in the system to complete the reaction at this space residence time. At the same time, the achieved level of styrene converted to the diol of 68 ± 4% indicates much better selectivity for the oxidation at the lower SO_5^{2-}: styrene ratio. It is worth mentioning here that maximum levels of conversion were generally smaller than those found in batch tests which can be explained by the deviation from the plug flow regime towards CSTR behaviour.

A constant concentration of the diol along the reactor can indicate that either the reaction is fast enough to be completed fully in the first reactor segment, or that the axial mixing is so efficient that the entire reactor system behaves as a single CSTR. The latter case is supported by the analysis of dimensionless numbers. However, to understand the experimental results better, RTDs were measured using standard tracer experiments and the results are shown in Fig. 8a and b. A tanks-in-series model was used for the comparison with the experimental response [20,26]:

$$f(\theta) = \frac{N(N\theta)^{N-1}}{(N-1)!}e^{-N\theta}$$

where f(θ) is RTD function and N is a number of tanks in series and $\theta = t/\tau$. A reasonable plug flow is achieved, when $N \geq 10$, while systems with $N < 10$ exhibit CSTR behaviour [20]. As it can be seen in Fig. 8a and b, the behaviour of OFR reactor was close to that of a sin-

gle CSTR when a displacement volume of 1.7 mL was applied. Minor deviations from single CSTR behaviour were observed when a displacement volume of 0.8 mL was tested, as indicated by the small difference between the modelled RTDs for CSTR (N = 1) and experimental results. It is worth noting that residence times calculated from the first moments of the RTDs (true residence times, τ, shown in Fig. 8) are considerably higher than the space residence times for P1–P4 points estimated from the total flow rate and volumes of the corresponding OFR segments, $t = V_R/u_\Sigma$ (from 1.1 to 1.3 times for four tubular OFR sections up to 4 times for a single OFR tube). Such inconsistency indicates significant deviation from the ideal CSTR behaviour due to a high degree of bypassing in the reactor which was more prominent for the shorter space residence times.

3.3.2. Oxidation at fast flow rates

In order to investigate the biphasic mixing and limitations of our OFR in greater detail, the dihydroxylation of styrene was performed at a shorter total space residence time of 20.8 min, corresponding to that of a single tubular reactor segment at slow flow rates (Table 1, entries 2 and 3). Three sets of oscillating conditions were studied: 8 Hz/1.7 or 0.8 mL and 5 Hz/1 mL. In the first two cases the corresponding Re_0s were left unchanged (5231 and 2615) but ψ were decreased to 394 and 197 respectively. These numbers indicate that the flow regime is still far from the plug flow [25,32]. For the latter case, the values are in middle of the transitional region (Re_0 = 1923 and ψ = 145) and St = 0.2 indicates good mixing inside the cavities. However, the performance of OFR cannot be described as pure CSTR which is further confirmed by the analysis of RTDs (Fig. 8c and d).

Droplet size distributions for two sets of the oscillating conditions measured during the oxidation are shown in Fig. 9c and d. Average droplet sizes along the reactor of 14 ± 2 μm for 8 Hz/1.7 mL and 16 ± 1 μm for 5 Hz/1 mL are close to those observed at the slower flow rates. This indicates that breakage of the dispersed phase inside the reactor is fast and efficient at this timescale and under these oscillating conditions. Under these conditions, conversions of styrene to the diol increased from sample port P0 to P4 along the reactor, reaching about 50% at the outlet of the reactor (see Fig. 10b) suggesting that slightly longer residence times would be necessary for the complete oxidation of styrene (see Fig. 10a, for comparison). At 5 Hz/1 mL, the estimated initial reaction rate of 1.2×10^{-4} M s^{-1} is close to that found in the case of batch membrane emulsification in the dispersion cell, i.e. there is virtually no mass-transfer limitation in the biphasic oxidation of the styrene for the droplet sizes below 16 μm.

Analysis of the RTDs (Fig. 8) reveals that the behaviour of the reactor is now different as evidenced from the changed shapes of the curves although it is still far from the ideal case of plug flow. Pure CSTR mixing was observed only at the shortest residence times (Fig. 8c and d). The number of CSTR equivalents, calculated for the 8 Hz/1.7 mL oscillatory conditions from the best fittings of the tanks-in-series model to the experimental data changes from N = 1 for a single tubular segment (tracer injected to P4), to N = 3 for the whole reactor rig (tracer injected to P0). The slightly better performance was observed at the milder oscillating conditions of 5 Hz and 1 mL displacement. The corresponding best fittings were obtained at N = 2 for a single tube to N = 5 for the whole reactor system, which are much lower than $N \geq 10$ required for a plug flow regime to be fulfilled [20]. This is a limitation of the current setup, but longer reactors could provide improved performance.

3.3.3. Oxidation with the integrated cross-flow membrane emulsification module

The other way to improve the performance of the system is to continuously generate the emulsion from the reaction mixture in a separate device (e.g. dispersion cell, cross-flow or azimuthally oscillating membrane emulsifier [16,24,36]) and pump it to the OFR at the same time. In this study, a cross-flow membrane module with the installed SPG tubular membrane (see Section 2.5 and Fig. 3) was integrated with the OFR and tested. Preliminary tests of the water-styrene system with added surfactant allowed a high degree of plug flow to be obtained at 5 Hz/0.4 mL and total space residence time of 20.8 min (see Fig. 8e). These oscillatory conditions correspond to St number of 0.44 indicating moderate mixing inside the cavities and Re_0 numbers from the transitional region (Re_0 = 865 and ψ = 65). Best fittings of the tanks-in-series model to the experimental results were obtained at N = 4 for a single tubular segment and N = 19 for the whole reactor system. The latter number indicates a plug flow operation regime which is established at residence times longer than 14 min.

However, at these oscillating conditions, it was not possible to achieve an appropriate mixing in a real biphasic reaction mixture during the oxidation in the OFR, even with the addition of 150 mg L^{-1} of surfactant in the aqueous phase. The process was severely affected by coalescence leading to phase separation and accumulation of styrene in the bubble-shaped segments of the OFR during the oxidation. In order to slow down the rate of coalescence, it is necessary to reduce average droplet size of the emulsion. This can be done by increasing the frequency and/or displacement of flow oscillations as shear stress at the surface of the membrane is proportional to $x_0 f^{3/2}$ [16]. On the other hand, the frequency/displacement must be low enough to achieve a plug flow regime. For this purpose, two sets of the oscillatory conditions were tested: 8 Hz/0.5 mL and 10 Hz/0.3 mL. The corresponding Re_0 and ψ are also in the middle of the transition region [25] (Re_0 = 1385 and 1038; ψ = 104 and 78, St = 0.44 and 0.74 respectively). The latter number indicates that there may be insufficient mixing inside the bubble-shaped segments of the OFR.

Droplet size distributions of samples taken from ports P0-P4 of the OFR during the oxidation and measured by ViPA are shown in Fig. 9e and f. Average droplet sizes of samples taken from the P0 sample port at the outlet of the membrane module are about 46 and 57 μm for 8 Hz/0.5 mL and 10 Hz/0.3 mL oscillatory conditions respectively. Average droplet sizes in the reactor are smaller, about 43 ± 3 μm and 43 ± 7 μm with a decreasing trend towards the outlet (indicated by standard deviations). The droplet sizes decreased along the OFR as expected due to the greater extent of styrene oxidation. A 47% yield of the diol and a selectivity of 0.8 was obtained at the outlet. This level of transformation of styrene into the water-soluble diol was calculated to result in a decrease of droplet sizes to about 42 μm, which is in a good agreement with the observed droplet sizes.

It can be seen in Fig. 10b, that conversions of styrene to the diol increase along the reactor, similar to those observed in the OFR at fast flow rates without the membrane module. Moreover, the rates of formation of the diol are similar for the OFR operated at 5 Hz/1 mL and the OFR integrated with SPG membrane module operated at 10 Hz/0.3 mL. This means that there are no significant mass transfer limitations in our biphasic system even for the droplet sizes below 60 μm. RTDs for the water-styrene system at 10 Hz/0.3 mL are shown in Fig. 8f. As it can be seen, it was possible to obtain a high degree of symmetry in RTDs at shorter residence times. Best fittings were obtained at N = 7 for a single tube (P3) and N = 12 for two tubes in series (P4) which are close to, or exceeding, the minimum number of STRs in series necessary for a plug flow operation regime. However, larger axial dispersions were observed for longer residence times (corresponding to tracer injections into P0-P2) evidencing the formation of stagnant zones due to insufficient mixing (as indicated by St = 0.74) and partial coalescence of styrene during continuous operation longer than 2 h. Best fittings of the tanks-in-series model to the experimental data were obtained at N = 5 for the injection to P2 (3 tubular reac-

tors in series) and N = 8 for P4 (4 tubular reactors in series) and P0 (total flow system of 5 tubular reactors in series) indicating that our system requires further improvement. In theory, this can be achieved by generating even smaller droplets as they coalesce at a much slower rate. Larger displacement volumes at 10 Hz provided a higher degree of mixing but led to the violation of the plug flow regime. An alternate way of size manipulation in emulsions is changing the membrane pore size [16]: smaller pore size SPG membranes allow smaller droplets to be generated at these oscillating conditions, and may possibly eliminate the problem of coalescence in the OFR. Another way to improve the performance of the system is to apply heating directly to the membrane module. In this case, the oxidation will start inside the membrane compartment and the formed diol will improve the stability of the dispersion.

3.4. Continuous extraction of the diol by ethyl acetate

Following the oxidation, it is necessary to separate the product from the aqueous phase, prior to regeneration of peroxodisulfate in the electrochemical cell. This can be done either by natural coalescence of the emulsion into two phases (if a product is insoluble in the aqueous phase) or by extraction of the product from the aqueous phase (if a product is water soluble). In the case of the styrene diol, it has limited solubility in the aqueous phase and acts as a surfactant to stabilise the droplets of other less soluble by-products such as 1-phenyl ethanol. Therefore, it is necessary to extract the product from the processed reaction mixture.

In preliminary batch tests, up to 98.6% of the diol can be extracted from the model reaction mixture (0.3 M diol and 1 M $(NH_4)_2SO_4$ dissolved in 2 M H_2SO_4), using ethyl acetate at 1:1 vol ratio (three extractions). Each extraction step required vigorous shaking of the aqueous phase with ethyl acetate and phase separation occurred within several seconds after the extraction. Therefore, similarly to the manual extraction, it is possible to extract the product continuously using an extra OFR section connected to the outlet of the reactor and equipped with the inlet for ethyl acetate (Fig. 4). In this case, the oscillations of flow at high frequency and/or displacement will provide excellent mixing of two immiscible phases, thus accelerating the extraction.

The corresponding continuous extractor (12 mL OFR with smooth periodic constrictions) was assembled and tested in the extraction of the diol from the model reaction mixture at 5 Hz and 1.2 mL displacement (see Section 2.6 for more details). As shown in Fig. 11, continuous extraction of the diol by ethyl acetate in the OFR was very fast and efficient. The amount of the extracted diol is virtually independent of the space residence time in the reactor and was affected only by the volume ratio of ethyl acetate to the aqueous phase. At the volume ratio of 0.5:1, the efficiency of the diol extraction was found to be about 85%. The increase of volume ratio from 0.5:1 to 2:1 led to a greater than 94% efficiency of extraction; higher organic phase ratios did not provide any significant improvement to the extraction process. However, the process may benefit from an additional extraction step for quantitative removal of the product from the downstream flow.

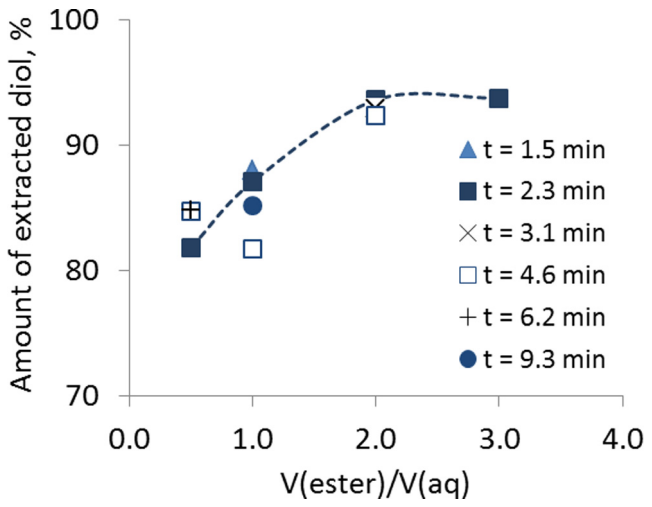

Fig. 11. Influence of volume ratio of ethyl acetate to the aqueous phase on the efficiency of the diol extraction from the model reaction mixture at different space residence times.

4. Conclusions

In this work, the feasibility of a continuous biphasic oxidation process has been demonstrated. It was shown that electrochemically generated peroxodisulfate is as effective as the commercially available equivalent oxidant. Significant benefits in using membrane emulsification in biphasic oxidations were demonstrated. Using a dispersion cell, mass-transfer limitations can be overcome, reducing the time scale of the reaction from several hours to less than 50 min. Subsequently, it was also shown that OFRs with smooth periodic constrictions can also facilitate the biphasic oxidation of styrene by the formation of unstable emulsions with a large interfacial area. Maximum conversions of styrene to the diol, of *ca.* 75% could be achieved in the OFR, which is comparable to the reaction performance in stirred batch reactors. An advantage of the OFR system is that it allows continuous operation with the productivity of ca. 0.5 mol day^{-1} and it can facilitate biphasic oxidation processes across a range of scales. RTD analysis showed that it was not possible to achieve plug flow regime using the OFR assembly, even at fast flow rates and smaller displacements/frequencies. Efficient mixing provided by high-frequency and large displacement volume oscillations is necessary for the formation of the unstable emulsions inside the OFR at the expense of plug flow regime.

Continuous membrane emulsification was successfully integrated with the OFR to perform biphasic oxidations. It was possible to achieve plug flow conditions at 5 Hz and 0.4 mL displacement for the water-styrene systems. However, these operating conditions were unsuitable for the biphasic reaction mixture containing persulfate and sulfuric acid due to the fast coalescence of styrene. Higher energy input provided by the frequency of 10 Hz and 0.3 mL displacement allowed continuous operation in plug flow regime at short residence times (for two tubes in series) when it was possible to obtain RTDs with N = 12. No mass-transfer limitations in the biphasic oxidation of styrene were observed when microdroplet sizes were less than 60 μm. However, long-term operation of the OFR-crossflow membrane assembly led to partial coalescence of styrene leading to the formation of stagnant zones in the reactor and violation of the plug flow regime. It is predicted that this drawback can be overcome by the generation of smaller droplets by smaller pore size tubular membrane, or by decoupled generation of emulsions at much higher shear stress. Further optimisation of the process and development of a predictive model for biphasic oxidations based on population balance and styrene oxidation mechanism are ongoing.

Finally, successful integration of an OFR with continuous extraction module will allow recirculation of the aqueous phase for the (electrochemical) regeneration of the oxidant, thus improving the atomic efficiency of the process. In extraction tests, more than 94% of diol can be extracted from the continuous phase in one pass. An additional extraction step may be necessary for quantitative extraction of the diol.

Acknowledgements

This work was supported by EPSRC (United Kingdom), grants [EP/L012278/1] and [EP/L011697/1].

References

[1] D.J.C. Constable, P.J. Dunn, J.D. Hayler, G.R. Humphrey, J.L. Leazer Jr., R.J. Linderman, K. Lorenz, J. Manley, B.A. Pearlman, A. Wells, A. Zaks, T.Y. Zhang, Key green chemistry research areas: A perspective from pharmaceutical manufacturers, Green Chem. 9 (2007) 411–420, http://dx.doi.org/10.1039/b703488c.
[2] P.T. Anastas, J.C. Warner, Green Chemistry: Theory and Practice, Oxford University Press, New York, 2000, 132 p.
[3] J.S. Carey, D. Laffan, C. Thomson, M.T. Williams, Analysis of the reactions used for the preparation of drug candidate molecules, Org. Biomol. Chem. 4 (2006) 2337–2347, http://dx.doi.org/10.1039/b602413k.
[4] P.L. Heider, S.C. Born, S. Basak, B. Benyahia, R. Lakerveld, H. Zhang, R. Hogan, L. Buchbinder, A. Wolfe, S. Mascia, J.M.B. Evans, T.F. Jamison, K.F. Jensen, Development of a multi-step synthesis and workup sequence for an integrated, continuous manufacturing process of a pharmaceutical, Org. Process Res. Dev. 18 (2014) 402–409, http://dx.doi.org/10.1021/op400294z.
[5] A. Pashkova, L. Greiner, Towards small-scale continuous chemical production: technology gaps and challenges, Chem. Ing. Tech. 83 (2011) 1337–1342, http://dx.doi.org/10.1002/cite.201100037.
[6] A. Kirschning, Chemistry in flow systems, Beilstein J. Org. Chem. 5 (2009) 15, http://dx.doi.org/10.3762/bjoc.5.15.
[7] J.A. Glaser, Good chemical manufacturing process criteria, Clean Technol. Environ. Policy 16 (2014) 1–7, http://dx.doi.org/10.1007/s10098-014-0725-8.
[8] V. Hessel, Process windows – gate to maximizing process intensification via flow chemistry, Chem. Eng. Technol. 32 (2009) 1655–1681, http://dx.doi.org/10.1002/ceat.200900474.
[9] J.C. Etchells, Process Intensification, Process Saf. Environ. Prot. 83 (2005) 85–89, http://dx.doi.org/10.1205/psep.04241.
[10] Filipe Gaspar, Marco Gil, Nuno Matos, Continuous Processing: Meeting the Need for New Manufacturing Strategies, Pharma's Alm. (2016).
[11] James. Bruno, Manufacturing in the 21st century: continuous flow chemistry has arrived, Am. Pharm. Rev. 17 (2014). http://www.americanpharmaceuticalreview.com/Featured-Articles/169309-Manufacturing-in-the-21st-Century-Continuous-Flow-Chemistry-has-Arrived/ (accessed December 25, 2016).
[12] C. Jiménez-González, P. Poechlauer, Q.B. Broxterman, B.S. Yang, D. Am Ende, J. Baird, C. Bertsch, R.E. Hannah, P. Dell'Orco, H. Noorman, S. Yee, R. Reintjens, A. Wells, V. Massonneau, J. Manley, Key green engineering research areas for sustainable manufacturing: a perspective from pharmaceutical and fine chemicals manufacturers, Org. Process Res. Dev. 15 (2011) 900–911, http://dx.doi.org/10.1021/op100327d.
[13] J. Zhu, K.K. Hii, K. Hellgardt, Toward a green generation of oxidant on demand: practical electrosynthesis of ammonium persulfate, ACS Sustainable Chem. Eng. 4 (2016) 2027–2036, http://dx.doi.org/10.1021/acssuschemeng.5b01372.
[14] S.M. Joscelyne, G. Trägårdh, Membrane emulsification – a literature review, J. Membr. Sci. 169 (2000) 107–117, http://dx.doi.org/10.1016/S0376-7388(99)00334-8.
[15] R.G. Holdich, M.M. Dragosavac, G.T. Vladisavljević, S.R. Kosvintsev, Membrane emulsification with oscillating and stationary membranes, Ind. Eng. Chem. Res. 49 (2010) 3810–3817, http://dx.doi.org/10.1021/ie900531n.
[16] R.G. Holdich, M.M. Dragosavac, G.T. Vladisavljević, E. Piacentini, Continuous membrane emulsification with pulsed (oscillatory) flow, Ind. Eng. Chem. Res. 52 (2013) 507–515, http://dx.doi.org/10.1021/ie3020457.
[17] A.W. Dickens, M.R. Mackley, H.R. Williams, Experimental residence time distribution measurements for unsteady flow in baffled tubes, Chem. Eng. Sci. 44 (1989) 1471–1479, http://dx.doi.org/10.1016/0009-2509(89)80023-5.
[18] M.R. Mackley, X. Ni, Mixing and dispersion in a baffled tube for steady laminar and pulsatile flow, Chem. Eng. Sci. 46 (1991) 3139–3151, http://dx.doi.org/10.1016/0009-2509(91)85017-R.
[19] X. Ni, Residence time distribution measurements in a pulsed baffled tube bundle, J. Chem. Technol. Biotechnol. 59 (1994) 213–221, http://dx.doi.org/10.1002/jctb.280590302.
[20] J.R. McDonough, A.N. Phan, A.P. Harvey, Rapid process development using oscillatory baffled mesoreactors – a state-of-the-art review, Chem. Eng. J. 265 (2015) 110–121, http://dx.doi.org/10.1016/j.cej.2014.10.113.
[21] T. McGlone, N.E.B. Briggs, C.A. Clark, C.J. Brown, J. Sefcik, A.J. Florence, Oscillatory Flow Reactors (OFRs) for continuous manufacturing and crystallization, Org. Process Res. Dev. 19 (2015) 1186–1202, http://dx.doi.org/10.1021/acs.oprd.5b00225.
[22] X. Ni, M.R. Mackley, A.P. Harvey, P. Stonestreet, M.H.I. Baird, N.V. Rama Rao, Mixing through oscillations and pulsations—a guide to achieving process enhancements in the chemical and process industries, Chem. Eng. Res. Des. 81 (2003) 373–383, http://dx.doi.org/10.1205/02638760360596928.
[23] E. Lobry, T. Lasuye, C. Gourdon, C. Xuereb, Liquid-liquid dispersion in a continuous oscillatory baffled reactor – application to suspension polymerization, Chem. Eng. J. 259 (2015) 505–518, http://dx.doi.org/10.1016/j.cej.2014.08.014.
[24] S.R. Kosvintsev, G. Gasparini, R.G. Holdich, I.W. Cumming, M.T. Stillwell, Liquid - Liquid membrane dispersion in a stirred cell with and without controlled shear, Ind. Eng. Chem. Res. 44 (2005) 9323–9330, http://dx.doi.org/10.1021/ie0504699.
[25] A.P. Harvey, M.R. Mackley, P. Stonestreet, Operation and optimization of an oscillatory flow continuous reactor, Ind. Eng. Chem. Res. 40 (2001) 5371–5377, http://dx.doi.org/10.1021/ie0011223.
[26] O. Levenspiel, Chemical Reaction Engineering, Wiley, 1999.
[27] I.M. Kolthoff, I.K. Miller, The chemistry of persulfate. I. The kinetics and mechanism of the decomposition of the persulfate ion in aqueous medium, J. Am. Chem. Soc. 73 (1951) 3055–3059, http://dx.doi.org/10.1021/ja01151a024.
[28] D.A. House, Kinetics and mechanism of oxidations by peroxydisulfate, Chem. Rev. 62 (1962) 185–203, http://dx.doi.org/10.1021/cr60217a001.
[29] P.C. Bulman Page, F. Marken, C. Williamson, Y. Chan, B.R. Buckley, D. Bethell, Enantioselective organocatalytic epoxidation driven by electrochemically generated percarbonate and persulfate, Adv. Synth. Catal. 350 (2008) 1149–1154, http://dx.doi.org/10.1002/adsc.200800064.
[30] S.D. Bishopp, J.L. Scott, L. Torrente-Murciano, Insights into biphasic oxidations with hydrogen peroxide; towards scaling up, Green Chem. 16 (2014) 3281, http://dx.doi.org/10.1039/c4gc00598h.
[31] S.D. Bishopp, A Solvent-Free Alternative for Green Liquid-Liquid Biphasic Oxidations Table of Contents, Bath University, 2014.
[32] M.S.R. Abbott, A.P. Harvey, G.V. Perez, M.K. Theodorou, Biological processing in oscillatory baffled reactors: operation, advantages and potential, Interface Focus 3 (2013) 20120036, http://dx.doi.org/10.1098/rsfs.2012.0036.
[33] A.P. Harvey, M.R. Mackley, T. Seliger, Process intensification of biodiesel production using a continuous oscillatory flow reactor, J. Chem. Technol. Biotechnol. 78 (2003) 338–341, http://dx.doi.org/10.1002/jctb.782.
[34] A.N. Phan, A.P. Harvey, M. Rawcliffe, Continuous screening of base-catalysed biodiesel production using new designs of mesoscale oscillatory baffled reactors, Fuel Process. Technol. 92 (2011) 1560–1567, http://dx.doi.org/10.1016/j.fuproc.2011.03.022.
[35] A.N. Phan, A.P. Harvey, Characterisation of mesoscale oscillatory helical baffled reactor—experimental approach, Chem. Eng. J. 180 (2012) 229–236, http://dx.doi.org/10.1016/j.cej.2011.11.018.
[36] P.S. Silva, M.M. Dragosavac, G.T. Vladisavljević, H.C.H. Bandulasena, R.G. Holdich, M. Stillwell, B. Williams, Azimuthally oscillating membrane emulsification for controlled droplet production, AIChE J. 61 (2015) 3607–3615, http://dx.doi.org/10.1002/aic.14894.